Structural Eng. / Earthquake Eng. Vol. 6. No. 2, 327s-336s. October 1989
Japan Society of Civil Engineers (Proc. of JSCE No. 410/I-12)

A STUDY ON THE FATIGUE DESIGN OF PARALLEL WIRE STRANDS ON CABLE-STAYED BRIDGES

By Shunichi NAKAMURA and Hajime HOSOKAWA***

A new type of parallel wire strands[1] were developed for stays on cable-stayed bridges. A strand consists of slightly helically twisted wires with high fatigue resistant sockets. The results of fatigue tests for these socketed cables were presented. A design non-dimensional S-N curve was proposed for these new cables. Stays may suffer considerable stress fluctuation when cables oscillate due to winds or vehicles on the bridge. Cable normal and secondary bending stresses due to the oscillation were obtained analytically with some consideration on the effect of support conditions. Fatigue lives due to random traffic were investigated by a simulation method for the three-span cable-stayed bridge. Cables show different fatigue lives depending on the position of the bridge and the shape of influence lines. A simple method was then proposed to predict fatigue damages and proved effective.

Keywords : cable-stayed bridges, cable fatigue, cable oscillation

1. INTRODUCTION

Cables play an crucial role on cable-stayed bridges : they connect girders and towers, therefore, the static and dynamic movement of girders and towers are simultaneously transferred into cables. Spiral strands or locked-coil strands have been favorably used for stays in U. K. and West Germany mainly because of easiness of handling, higher damping and anti-corrosion properties. However, there have been a couple of improvements on parallel wire strands for the last ten years or so. Parallel wire strands with epoxy resin and steel ball filled sockets (termed Hi-Am anchor) were developed in Germany and showed a better fatigue resistance than spiral strands[2]. Another type of parallel wire strands with epoxy resin and Zn-Cu alloy filled sockets (termed NEW-PWS) were developed[1] in Japan. A strand is coated by polyethylene at a factory, which eliminates laborious field coating works. Because of these new advances parallel wire strands have become popular in Japan and other countries as well.

Although the importance of cable fatigue strength has been acknowledged since early, fatigue tests of the prototype socketed cables are difficult technically and financially because of their size which requires large experimental facilities, consequently there have not been many data so far. Therefore, fatigue tests with NEW-PWSs were carried out to obtain further data and the results were presented in 2 of the present paper.

It is sometimes observed that stays on cable-stayed bridges oscillate due to winds, which naturally causes stress fluctuations. Vortex shedding, galloping and buffeting are the most common phenomena of cable vibration. Wake galloping also occurs when two cables are closely placed. Another type of cable oscillation was observed on the Nagoya Harbour West Bridge[3]. The oscillation was termed 'rain

* Member of JSCE, Ph. D., Nippon Steel Corporation (2-6-3 Otemachi, Chiyoda-ku, Tokyo 100)
** Bridge Engineering and Construction Division, Nippon Steel Corporation (2-6-3 Otemachi, Chiyoda-ku, Tokyo 100)

vibration', because it was observed only on rainy days with wind speed about 10 m/sec. The maximum amplitude observed was about 25 cm. Normal and secondary bending stress ranges and fatigue sensitivity caused by such oscillation was studied with some consideration on the effect of cable support in 3.

A fatigue problem have not been reported in main cables of suspension bridges except the inclined hangers[4], whereas, there may be a significant fatigue effect for stays on cable-stayed bridges[5] because of the shape of influence lines of cable tension which has both positive and negative areas which cause relatively large stress amplitudes. The stress fluctuations due to random traffic was obtained by a simulation method using a model day traffic which was derived from several traffic data on major roads in Japan. A simple method was then proposed to predict a fatigue damage and compared with the results calculated by the simulation method in 4.

2. FATIGUE TESTS ON NEW PARALLEL WIRE STRANDS

Fig. 1 is a typical cross section of new parallel wire strands[1]. Wires are socketed by 98 % Zn and 2 % Cu which is the most common and reliable materials to pour. However, they require rather high pouring temperature about 460°C and may reduce the fatigue strength. Due to the fact that most of the fatigue damages occur near the entrance of sockets, epoxy resin which does not require high pouring temperatures is used around the neck of sockets to reduce secondary bending stresses. Wires are helically twisted within the angles not to reduce elastic modulus in order to hold a strand shape and to make its handling easy.

Static and fatigue tests with five NEW-PWSs were carried out. Test pieces were 2.5 metre long, consisted of 139 wires of 7 mm diameter, and twisted with angle of 3.5 degrees. The ultimate static strength of wires was provided for ranges 1 568 N/mm^2 to 1 764 N/mm^2, and the elastic modulus were more than 1.96×10^5 N/mm^2. Test cables were excited cyclically by the fatigue test machine with capacity of 400 tonf. Accelerators were attached to the sockets during the tests in order to detect a wire breakage by catching an impulse which occurs when wires break.

Table 1 is the fatigue test results carried out this time and previously[1]. Cables used for the previous fatigue tests[1] were socketed with the same materials as this time, but wires were purely parallel. However, we could not find significant differences between both results. Stress ranges were between 196 and 343 N/mm^2, and total cycles were between 0.52 to 5 million times. The wire breakages were considerably small and occurred both inside and outside sockets. Broken wire percentage of most strands is less than 5 %, which can be taken safe enough from a practical viewpoint. These test data are plotted in Fig. 2, where non-dimensional stress range S is used. S is expressed by σ : stress range, σ_u : ultimate strength and σ_M : mean stress.

$$S=(\sigma/\sigma_u)/\{1-(\sigma_M/\sigma_u)^2\} \quad \cdots\cdots (1)$$

This non-dimensional expression was proved to be efficient for spiral strands in the previous study[4),5)]. The following relationship can be conservatively assumed as design S-N curve for NEW-PWSs from

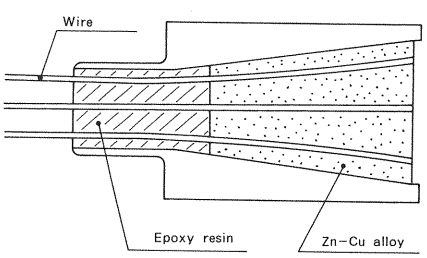

Fig. 1 Cross section of a NEW-PWS socket.

Table 1 Fatigue test results of NEW-PWSs.

No.of wires	stress ranges	mean stress	S	cycles (x10^4)	percentage of broken wires and broken parts
139	196	529	.141	200	0.7% inside socket
139	196	529	.141	500	0%
139	245	505	.174	225	2.2% inside socket
139	294	480	.207	100	6.6% inside/outside socket
139	294	480	.207	103	8.6% inside socket
127*	196	529	.141	504	0%
127*	196	529	.141	206	0%
127*	245	505	.174	210	2.4% inside socket
127*	245	505	.174	244	2.4% inside socket
127*	343	456	.239	52	1.6% outside socket
91*	294	480	.207	200	1.1% outside socket

* indicates test data carried out previously[1]
Wires are all 7 mm diameter. Unit of stresses is N/mm^2

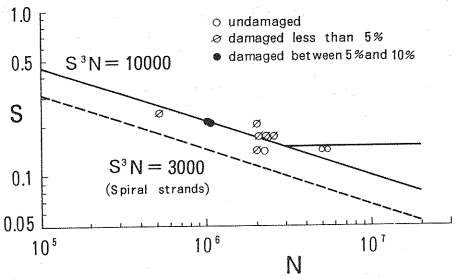

Fig. 2 Design S-N curve for NEW-PWSs.

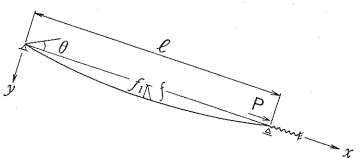

Fig. 3 A model of a stay on the bridge.

Fig. 2.

$S^3N = 10\,000$ ..... (2)

There may be a lower limit of stress ranges under which no fatigue occurs, however, it can not be verified because of insufficient data of cycles over 2×10^6. A S-N relationship for spiral strands[4),5)] is also shown in Fig. 2. It is obvious that parallel wire strands have better fatigue resistance than spiral strands. It should be reminded that we need more data to improve the accuracy of the proposed S-N curve especially in order to investigate the socket size effects.

Test wires were statically tensioned after the fatigue tests. No reduction of ultimate strength was observed compared with virgin cables. Cable length was also measured before and after the fatigue tests, showing that cable elongation including creep of both sockets was small and ranged form 0.8 mm to 1.3 mm.

3. STRESS FLUCTUATION DUE TO CABLE OSCILLATION

Fig. 3 is an analytical model of an inclined cable with an end spring which represents girder and tower flexibilities. A parabolic shape is assumed for a cable configuration along the inclined axis when a cable carries dead loads. Cables with small sag to span ratio were studied in this paper due to the fact that a sag of stays is very small on existing cable-stayed bridges. Therefore, it is assumed that inclined cables can be expressed by cable deflections perpendicular to the inclined axis. f_1 is a sag defined perpendicular to the inclined axis and it relates a sag f measured vertically.

$f_1 = f\cos\theta$ ..... (3)

Initial force along the inclined axis T_0 is expressed by :

$T_0 = mg\cos\theta\, l^2/8f_1$ ..... (4)

where m is a mass per unit cable length, l : cable length and θ : inclined angle. m equals ρA_c, where ρ : mass per unit volume, g : gravity acceleration and A_c : cable sectional area. ρ was set at 7 850 kg/m^3 in this study. Elongation of cable is the sum of cable length due to geometric deformation and spring length change[4),15)] :

$$T\,L_e/E_c\,A_c - 8f_1/l^2\int_0^l w\,dx - (P-T)/k = 0 \quad \cdots\cdots (5)$$

where,

$$L_e = \int_0^l \{1+(dy/dx)^2\}^{3/2}\,dx \simeq l(1+8f_1^2/l^2) \quad \cdots\cdots (6)$$

T : additional cable tension due to oscillation, w : cable deflection perpendicular to the inclined axis, E_c : cable elastic modulus, k : end spring constant and P : external force. If $P=0$, we have :

$$T = 8f_1\int_0^l w\,dx/l^2 r \quad \cdots\cdots (7)$$

where,

$r = L_e/E_c\,A_c + 1/k$ ..... (8)

Natural circular frequencies of an inclined cable ω can be obtained by the energy principle. Expressing

cable deflection w by sinusoidal terms, kinetic energy T_e, cable potential energy V_e and spring potential energy K_e are obtained as follows.

$$\left.\begin{aligned} w&=\sum_i a_i \sin(i\pi x/l)\\ T_e&=\frac{1}{2}m\omega^2\int_0^l w^2dx=\frac{1}{4}ml\omega^2\sum_i a_i^2\\ V_e&=\frac{1}{2}T_0\int_0^l(dw/dx)^2dx+\frac{4f_1T}{l^2}\int_0^l wdx=\frac{mg\pi^2l}{32f_1}\sum_i(ia_i)^2+\frac{128f_1^2}{r\pi^2l^2}\{\sum_i(a_i/i)\}^2\\ K_e&=\frac{k}{2}dx^2=\frac{T^2}{2k}=\frac{128f_1^2}{k(lr\pi)^2}\{\sum_i(a_i/i)\}^2 \end{aligned}\right\}\quad\cdots\cdots(9)$$

By the energy principle $\partial(T_e-V_e-K_e)/\partial a_i$ should be zero, which leads the following eigen value equation.

$$\begin{Bmatrix} a_1\\ a_3\\ a_5\\ a_7\\ a_9 \end{Bmatrix}\omega^2=\begin{bmatrix} F_2+F_3 & F_3/3 & F_3/5 & F_3/7 & F_3/9\\ F_3/3 & 9F_2+F_3/9 & F_3/15 & F_3/21 & F_3/27\\ F_3/5 & F_3/15 & 25F_2+F_3/25 & F_3/35 & F_3/45\\ F_3/7 & F_3/21 & F_3/35 & 49F_2+F_3/49 & F_3/63\\ F_3/9 & F_3/27 & F_3/45 & F_3/63 & 81F_2+F_3/81 \end{bmatrix}\begin{Bmatrix} a_1\\ a_3\\ a_5\\ a_7\\ a_9 \end{Bmatrix}\quad\cdots\cdots(10)$$

where, $F_1=ml/2$, $F_2=\pi^2mgl/16f_1F_1$ and $F_3=256f_1^2(1/r+1/kr^2)/\pi^2l^2F_1$. We are interested in only odd numbers of a_i because no cable stress occurs in asymmetric modes. Fourier terms up to 9 were found to be sufficient for the present study, but more terms could be easily extended. An additional normal stress range σ_N due to oscillation is obtained from eq. (7) and eq. (9).

$$\sigma_N=T/A_c=16f_1(a_1+a_3/3+a_5/5+a_7/7+a_9/9)/\pi lrA_c\quad\cdots\cdots(11)$$

Fig. 4 shows natural circular frequencies ω versus f_1/l in the first two symmetric modes with dotted lines of natural circular frequencies calculated by the simple string theory. Inclined angle of 30 degrees, cable length of 200 m, k/A_c of 6 N/mm³ and a/l of 0.01 (a : amplitude) were set in this figure. It is understood that both results are nearly equal when f_1/l is small, whereas, the difference becomes large when f_1/l are large and consequently mode shapes become like higher symmetric modes. This phenomena, namely the existence of modal crossover, has been found by many researchers[6].

Fig. 5 shows σ_N of first two symmetric modes versus spring constant attached to cable ends. Inclined angle of 30 degrees, cable length of 200 m, f_1/l of 0.005 and a/l of 0.01 were set. It is understood that σ_N increases with k/A_c but saturates around $k/A_c=10$. It is reminded that k/A_c usually ranges between 5 to 10 N/mm³ on existing bridges, therefore, it is important to include the effect of girder and tower flexibilities in evaluating cable stresses. On the other hand, it was found that natural frequencies do not

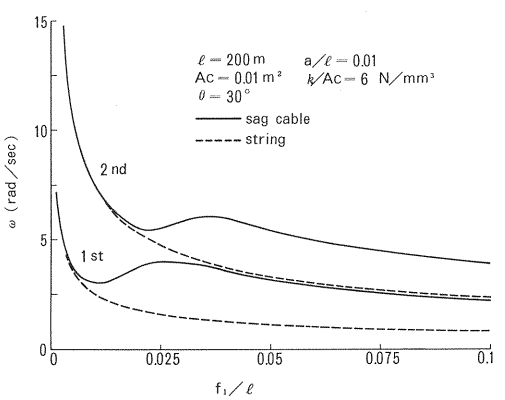

Fig. 4 First and second natural frequencies.

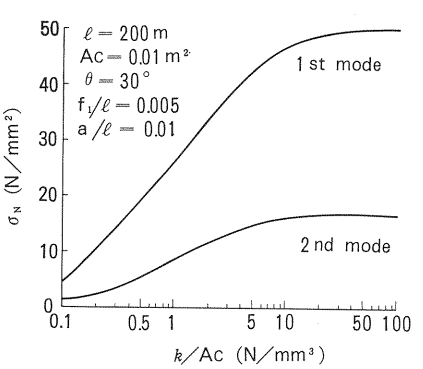

Fig. 5 Normal stresses versus k/A_c in the first and second symmetric modes.

depend on k/A_c and remain almost constant.

When a socket is pin-connected to girders or towers and rotate freely, cables have no bending stresses at sockets, whereas, sockets are usually fixed in its rotation on actual structures, and secondary bending stresses occur at the cable end[12]. A sine curve is assumed to express cable mode configuration as illustrated in Fig. 6(a), and this assumption does not spoil the accuracy in obtaining basic dynamic cable behaviours such as vibration modes and natural frequencies. However, modification should be made to include local end effects, because a cable is flat at its end as shown in Fig. 6(b), which causes an end moment M_B.

$$M_B=2EI_c\theta_B/l \quad \cdots\cdots (12)$$

where,

$\theta_B=(a_1+3a_3+5a_5+7a_7+9a_9)\pi/l$

θ_B is an end rotation angle. I_c is cable moment of inertia, which depends on friction between wires in a strand. When there is no friction, I_c is the sum of individual wire inertia. However, when there is sufficient friction between wires, a strand behaves like a bar consisting of whole wires. The latter gives severer secondary bending stresses, and was used for I_c in this calculation.

Normal and secondary bending stresses, σ_N and σ_B, in the first symmetric mode is shown in Fig. 7. σ_N increases proportionally until f_1/l of 0.02, however, it decreases afterwards. This is due to a common cable mode transition phenomena that cable symmetric mode change from a pure sine curve to a more complex configurations, which was already mentioned in the comment on Fig. 4. σ_B is much smaller than σ_N, although it becomes more important for short and rigid cables. It is reminded that, in spite of the non-linear behaviours of σ_N and σ_B, f_1/l is under 0.01 on existing bridges, and σ_N and σ_B can be treated linear versus f_1/l in practical cases. It should be reminded that cables with only small sag to span ratio can be expressed precisely by the aforementioned equations, and errors may increase for inclined cables with large sag to span ratio. However, this theory is adequate as far as it is used for stays on cable-stayed bridges.

Cable fatigue damage D is evaluated by Miner's rule, using S-N relationship of Fig. 2.

$$D=\frac{N}{10\,000}\left\{\frac{\sigma/\sigma_U}{1-(\sigma_D/\sigma_U)^2}\right\}^3 \quad \cdots\cdots (13)$$

where, σ is a total stress range consisting of σ_N and σ_B. If σ_U is 1 568 N/mm^2 and σ_D is 0.25 σ_U, fatigue damage is 1.0 when σ is 251, 147, and 68 N/mm^2 for cycles of 2×10^6, 10^7 and 10^8 respectively. Take an inclined cable with l of 200 m, θ of 30°, A_c of 0.01 m^2 and k/A_c of 6 N/mm^3, as shown in Fig. 8 where stress ranges were obtained versus oscillation amplitudes for different sag to span rations. It is understood from Fig. 8 that allowable amplitudes are 2.56, 1.50 and 0.69 metres when N are 2×10^6, 10^7 and 10^8 for $f_1/l=0.01$. Let us take an example to demonstrate the possibility of a fatigue problem. If a cable vibrates with period of 0.72 sec by certain wind speed, and lasts for 4 hours per day, and 50 days per year, the total cycles of stress fluctuations is 10^8 times for 50 years. Therefore, if an amplitude of cable vibration exceeds 0.69 m, a fatigue failure could result. It should be reminded that secondary bending fatigue strength is assumed to be similar to axial fatigue

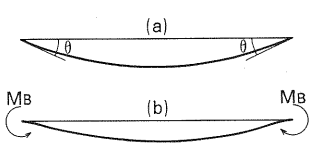

Fig. 6 Secondary end moments.

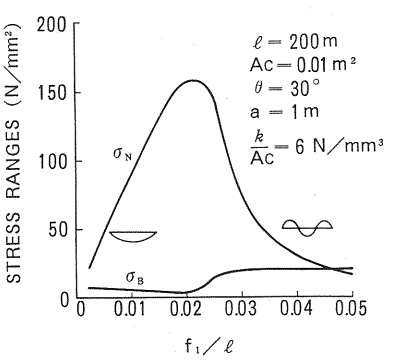

Fig. 7 Stress ranges in the first mode.

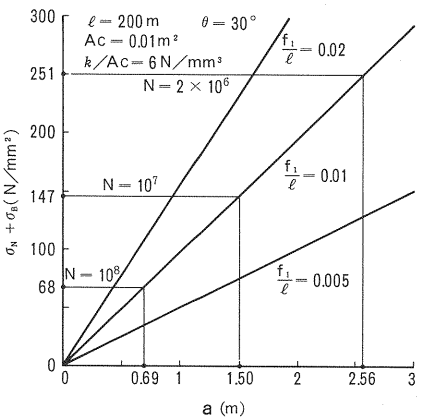

Fig. 8 Total cable stresses and fatigue lives.

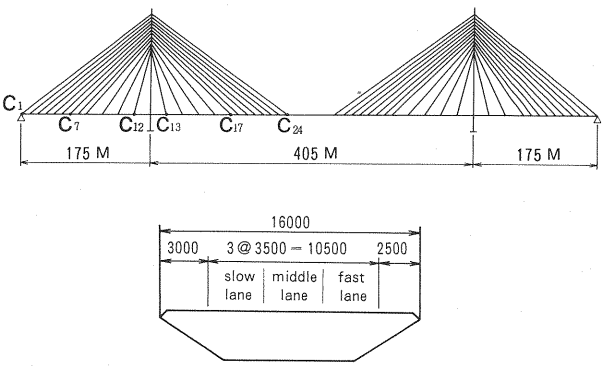

Fig. 9 Layout and cross section of the model cable-stayed bridge.

strength in eq. (13), although a further experimental study will be required for the validation.

4. FATIGUE DAMAGE DUE TO RANDOM TRAFFIC

(1) Evaluation of fatigue damage by a simulation method

A fatigue problem on spiral strands caused by random traffic flows was studied by a Monte Carlo simulation method in the previous paper[5]. A similar approach was applied to evaluate the fatigue strength of parallel wire strands on cable-stayed bridge using model traffic flow estimated by current Japanese traffic data. The Nagoya Harbour West Bridge[7] as shown in Fig. 9, a three continuous span cable-stayed bridge with 12 cables per fan in double cable planes, was taken as example to study because the bridge has one of the most flexible girder so far in Japan. Flexible girders would be more likely to cause cable fatigue damage than stiffer girders according to the previous study[5]. The effect of secondary bending stresses near socket entrance was also taken into account.

Table 2 is a model day traffic used in the paper. This model was derived from the relevant studies[8)~11)] on traffic surveys on major Japanese roads. A three lane single carriageway was assumed. The total number of traffic of this model in a day is 75 400, which is nearly equivalent to the busiest highway data in Japan. Traffic was classified into three groups : congested (group A), daytime (group B) and night traffic (group C). Vehicle speed v was assumed 20, 60 and 70 km/h for traffic group A, B and C respectively. Three types of vehicles were used in this study as shown in Table 3 : heavy goods vehicles (HGVs), light goods vehicles (LGVs) and private vehicles (PRVs). The probabilistic distribution of LGVs and PRVs was assumed normal distribution, whereas, that of HGVs was found to be more like log-normal distribution[10].

Third order Erlan distribution was assumed for arriving time interval probabilistic distribution function $f(t)$.

$$f(t)=\lambda e^{-\lambda t}(\lambda t)^2/2 \quad \cdots\cdots (14)$$

where, $\lambda=3\,Q/3\,600$, Q : hourly traffic volume and t : arriving time interval. A series of vehicles, with different arriving intervals, vehicle types, and weight, was simulated by Monte Carlo method for each lane based on the model traffic data.

When sockets are unable to rotate in girders and towers, secondary bending stresses occur at cable ends when girders deflect. Bending stress σ_B is obtained by the following Wyatt's theory[12] :

$$\sigma_B=2\,w_E\sqrt{E_c\sigma_D} \quad \cdots\cdots (15)$$

where, w_E : end rotation angle of girder and σ_D : dead load stress.

Stress histories of σ_N and σ_B are obtained by moving a series of live loads on the normal and bending

Table 2 Model traffic data.

traffic group	congested A	daytime B	night C
duration (h)	6	10	8
proportion of HGVs (%)	5	10	30
proportion of LGVs (%)	20	30	30
proportion of PRVs (%)	75	60	40
Q_1	2000	1500	700
λ_1	1.67	1.25	.583
Q_2	1500	1000	300
λ_2	1.25	.834	.25
v	20	60	70
total volume in a year	27 521 000		

Q_1, Q_2: Hourly traffic volume in slow and two fast lanes respectively, $\lambda_1/3$, $\lambda_2/3$: Average arriving vehicles in a second in slow and two fast lanes respectively, v: vehicle speed (km/h)

Table 3 Model vehicles.

(unit : kN)

traffic group	distribution function	mean weight	standard deviation	maximum weight	minimum weight
HGV	Log-normal	196.0	78.4	686	78.4
LGV	Normal	49.0	27.4	294	9.8
PRV	Normal	15.7	7.8	49	2.0

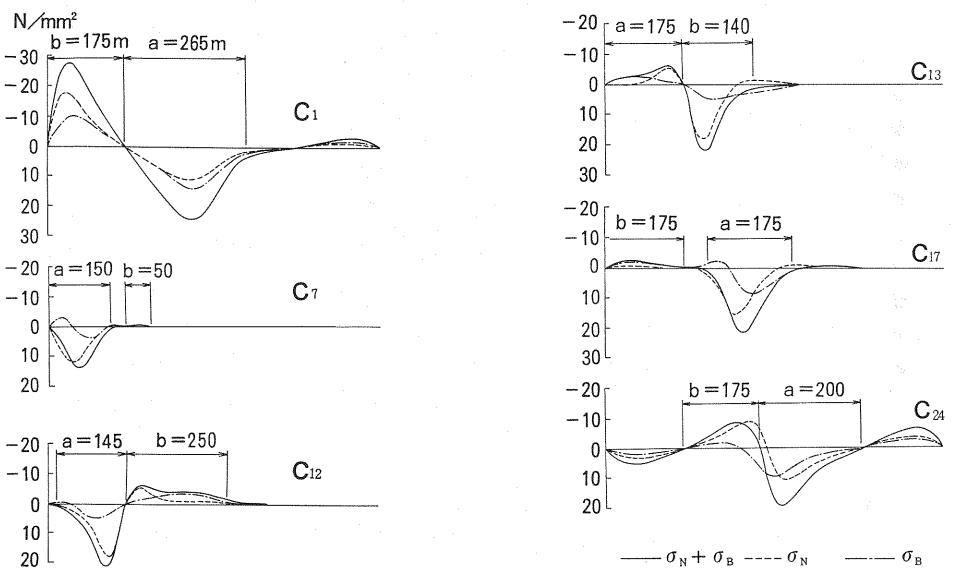

Fig. 10 Influence lines of cable stresses due to a 196 kN HGV.

stress influence lines in Fig. 10. These stress influence lines are due to a 196 kN HGV in lane 1. Simulation time was 45 minutes. Intensity and cycles of stress ranges were then calculated by the reservoir method. Fatigue lives were finally obtained using Miner's rule.

Table 4 shows fatigue damages due to three traffic groups for six stays whose positions are indicated in Fig. 9. Fatigue damages for each cable estimated are not very different in three traffic groups. The yearly damage of anchor stay C_1 is maximum among the selected cables, with the value less than 0.01 which gives a fatigue life of more than 100 years. Other stays have lower fatigue damages and are pretty safe.

(2) Evaluation of fatigue damages by a simplified method

A simple method is proposed to predict fatigue damages instead of using simulation technique which usually requires time consuming works. Only one type of vehicle is used to evaluate fatigue damages. A HGV is chosen as representative vehicle because it gives major damages among all other types of vehicles.

Table 4 Fatigue analysis results.

cable no.	traffic group	SIMULAION D (/10^7)	SIMULAION Dyear (/100)	SIMPLIFIED METHOD a (m)	b (m)	c	Ds (/10^7)	Dsyear (/100)	Dyear / Dsyear
C_1	A	5.375					10.874		
	B	6.117	0.6754	265	175	1.12	8.364	1.1164	1.65
	C	5.669					10.063		
C_7	A	0.152					0.159		
	B	0.150	0.0173	150	50	0.05	0.109	0.0150	0.87
	C	0.142					0.131		
C_{12}	A	0.751					0.875		
	B	0.777	0.0982	145	250	0.35	0.762	0.0989	1.01
	C	0.801					0.931		
C_{13}	A	0.712					0.905		
	B	0.699	0.0849	140	175	0.35	0.727	0.0965	1.14
	C	0.775					0.891		
C_{17}	A	0.663					0.977		
	B	0.652	0.0755	175	175	0.15	0.706	0.0959	1.27
	C	0.628					0.849		
C_{24}	A	1.391					1.765		
	B	1.181	0.1514	200	175	0.43	1.304	0.1762	1.16
	C	1.368					1.572		

D,Ds:fatigue damage in 45min. Dyear,Dsyear:yearly fatigue damage

The equivalent cycles of a representative vehicle in lane i, N_{Ri}, is obtained so that it gives the same fatigue damage caused by all types of vehicles.

$$N_{Ri}=\sum_j W_{ij}^3 N_{ij}/W_R^3 \quad \cdots\cdots (16)$$

where, W_{ij} and N_{ij} are the average weight and number of vehicles of traffic group j in lane i for a simulation time. W_R is the average weight of the representative vehicle, namely 196 kN. It is understood from eq. (2) that fatigue damages are proportional to the third power of stress ranges. Fatigue damages D_i due to single representative vehicle in lane i can be easily calculated by maximum stress ranges of the influence lines in Fig. 10.

The total fatigue damage D can be then obtained, taking multi-vehicle effects C_{Mi} in lane i and multi-lane effects C_L:

$$D=C_L(C_{M1}D_1+C_{M2}D_2+C_{M3}D_3) \quad \cdots\cdots (17)$$

C_{Mi} takes account of the effects that more than one vehicles exist in lane i, and C_L the effect that a vehicle exists in other lanes. Wyatt and Nakamura[5] evaluated these coefficients by simulation and Fujino et al.[13),14)] obtained C_M analytically but used simulation for C_L.

Following four load cases were considered in evaluating C_L.

case 1 : a vehicle exists only in lane 1 (slow lane)

case 2 : vehicles exist only in lane 1 and lane 2 (middle lane)

case 3 : vehicles exist only in lane 1 and lane 3 (fast lane)

case 4 : vehicles exist in all three lanes

Each influence line of cable stresses is simplified, as shown in Fig. 11, by two sine curves with different peak values (1 and c) and different base lengths (a and b). Probabilities of the above four cases p_i are then obtained as follows.

$$\left.\begin{aligned} p_1&=\{N_{R1}-(L/L_0)N_{R2}\}\{N_{R1}-(L/L_0)N_{R3}\}/N_{R1}^2\\ p_2&=(L/L_0)N_{R2}\{N_{R1}-(L/L_0)N_{R3}\}/N_{R1}^2\\ p_3&=\{N_{R1}-(L/L_0)N_{R2}\}(L/L_0)N_{R3}/N_{R1}^2\\ p_4&=(L/L_0)^2 N_{R2}N_{R3}/N_{R1}^2 \end{aligned}\right\} \quad \cdots\cdots (18)$$

where, L is the total base length of simplified influence lines and L_0 is the total bridge span. We assume that a representative vehicle is at the peak position in lane 1, as indicated in Fig. 11, and another vehicles exist anywhere on the influence line with equal probability. C_L can be obtained by integrating all probabilities, assuming fatigue damages are proportional to the third power of stress ranges. C_L should include the effects of the above four load cases.

$$C_L=1.0\,p_1+p_2\int_0^L\left\{1+k_2\left(\sin\frac{\pi x_1}{a}-c\sin\frac{\pi x_2}{b}\right)\right\}^3 dx/L$$
$$+p_3\int_0^L\left\{1+k_3\left(\sin\frac{\pi x_1}{a}-c\sin\frac{\pi x_2}{b}\right)\right\}^3 dx/L$$
$$+p_4\int_0^L\int_0^L\left\{1+k_2\left(\sin\frac{\pi x_1}{a}-c\sin\frac{\pi x_2}{b}\right)\right.$$
$$\left.+k_3\left(\sin\frac{\pi y_1}{a}-c\sin\frac{\pi y_2}{b}\right)\right\}dx\,dy/L^2$$

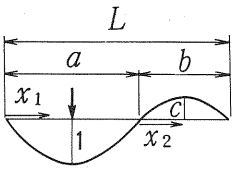

Fig. 11 Simplified influence line.

$$=p_1+p_2\{L+1.91\,k_2(a-bc)+1.5\,k_2^2(a-bc^2)+0.42\,k_2^3(a-bc^3)\}/L+p_3\{L+1.91\,k_3(a-bc)$$
$$+1.5\,k_3^2(a-bc^2)+0.42\,k_3^3(a-bc^3)\}/L+p_4\{L^2+1.91(k_2+k_3)L(a-bc)+1.5(k_2^2+k_3^2)L(a+bc^2)$$
$$+2.43\,k_2k_3(a-bc)^2+0.95\,k_2k_3(k_2+k_3)(a-bc)(a+bc^2)+0.42(k_2^3+k_3^3)L(a-bc^3)\}/L^2\cdots\cdots\quad(19)$$

Stress ranges due to vehicles in lane 2 and 3 are smaller than those in lane 1, and k_1 and k_2 are the relevant reduction coefficients.

Multi-vehicle effects C_M can be obtained by summing up the following three vehicle loading cases. Up to three vehicles in a lane at the same time was considered in this study.

case 1 : exactly one vehicle exists in a lane

case 2 : exactly two vehicles exist in the same lane

case 3 : exactly three vehicles exist in the same lane

Probability of case 1, q_1, is obtained so that, when a vehicle moves on the total base length L, next vehicle does not arrive during the corresponding time t_0 which is defined by L/v.

$$q_1=\int_{t_0}^{\varphi} f(t)dt=\lambda^2 e^{-\lambda t_0}(t_0^2+2\,t_0/\lambda+2/\lambda^2)/2\cdots\cdots\quad(20)$$

It was assumed that the effect of number of vehicles more than four could be included in case 3 and would not create significant errors. Probability of case 2, q_2, is obtained so that, while the first vehicle moves on the base length L, the second vehicle arrives during the time t which must be less than t_0, and the third vehicle does not arrive 0 and t_0-t.

$$q_2=\int_0^{t_0} f(t)\left\{\int_{t_0-t}^{\varphi} f(t)dt\right\}dt=\lambda^5 e^{-\lambda t_0}t_0^3(t_0^2/120+t_0/24\,\lambda+1/6\,\lambda^2)\cdots\cdots\quad(21)$$

The rest is the probability of case 3, q_3.

$$q_3=1-q_1-q_2\cdots\cdots\quad(22)$$

Suppose a vehicle is at the peak position as illustrated in Fig. 11, C_M is obtained in a similar way as C_L, assuming that other vehicles exist anywhere on the base length L with equal probability.

$$C_M=1.0\,q_1+q_2\int_0^L\left(1+\sin\frac{\pi x_1}{a}-c\sin\frac{\pi x_2}{b}\right)^3 dx/L+q_3\int_0^L\int_0^L\left(1+\sin\frac{\pi x_1}{a}-c\sin\frac{\pi x_2}{b}\right.$$
$$\left.+\sin\frac{\pi y_1}{a}-c\sin\frac{\pi y_2}{b}\right)^3 dxdy/L^2=q_1+q_2\{4.83\,a+b(1-1.91\,c+1.5\,c^2-0.42\,c^3)\}/L$$
$$+q_3\{13\,a^2+(9.66-10.54\,c+4.9\,c^2-0.84\,c^3)ab+b^2(1-3.82\,c+5.43\,c^2-2.74\,c^3)\}/L^2\cdots\cdots\quad(23)$$

As C_M is different for each lane with different v_i, C_{Mi} is defined by C_M for lane i.

The dimensions of the simplified influence lines are shown in Fig. 10 and Table 4, where fatigue damages estimated by this new method is compared with the simulated results. The difference due to both methods is largest for anchor cable C_1, which may be caused by the presence of the third significantly large peak of the influence line. In addition, as the base length of C_1 is larger than other cables, the presence of fourth vehicle may affect more significantly. However, the difference for other stays are mostly within 20 %, therefore, this new method is accepted satisfactory as a simple fatigue damage evaluation method. It would improve the accuracy of this analysis if we include the effect of the fourth vehicle, and use three peak sine curves to describe the influence lines.

5. CONCLUSION

A fatigue strength of newly developed parallel wire strands and the fatigue design method on cable-stayed bridges was studied experimentally and analytically as well. Main results and discussions are as follows.

(1) NEW-PWS, a parallel wire strand with Zn-Cu alloy and epoxy resin filled sockets, was proved to have better fatigue resistance than spiral strands. A design S-N curve was also proposed. The basic properties, elastic modulus, ultimate strength and elongation of strands did not change much after fatigue tests.

(2) Stress ranges and natural frequencies of an inclined cable with an elastic support at the cable end due to cable oscillation were calculated by the energy method. Secondary bending stresses were also obtained analytically. Taking a 200 metre long cable as example, the fatigue strength due to different oscillation amplitudes were studied. It was found that cable stresses are influenced by spring intensity. Once cable begins to vibrate, it takes considerable time to diminish, therefore, oscillations may cause a fatigue problem.

(3) Fatigue damages of stays on a cable-stayed bridge were obtained by the simulation method using a model day traffic. Anchor stay is the most sensitive among all cables, and should be carefully designed. An analytical method was developed to estimate fatigue by simplifying influence lines with two sine curves with different base lengths and peak values. The new method was found to produce close results obtained by the simulation method, and would be useful in practical fatigue design.

Finally, the authors appreciate the useful comments given by the reviewers of this paper.

REFERENCES

1) Tawaraya, Y., Hojyo, T., Konno, S. and Eguchi, T. : Mechanical properties of NEW-PWS on cable-stayed bridges, Seitetsu Kenkyu, No. 324, pp. 89-96, Jan. 1987 (in Japanese).
2) Birkenmaier, M. : Fatigue resistant tendons for cable-stayed construction, IABSE Proceedings, p-30/80, pp. 65-78, May 1980.
3) Kawahito, T. et al. : Characteristics of rain vibration of stays on cable-stayed bridges, Proceedings of 40 th annual conference of JSCE, pp. 429-430, Sep. 1985 (in Japanese).
4) Nakamura, S. and Wyatt, T. A. : Economical computation of stress histories in suspension bridge elements, with special reference to inclined hangers, Steel Structures Advances, Design and construction, pp. 118-127, Elsevier Applied Science, July 1987.
5) Wyatt, T. A. and Nakamura, S. : On the cable fatigue sensitivity of multi-stayed bridges, International conference on cable-stayed bridges, Bangkok, pp. 621-632, Nov. 1987.
6) Yamaguchi, H. and Fujino, Y. : Modal damping of flexual oscillation in suspended cables, Structural Eng. /Earthquake Eng., Vol. 4, No. 2, pp. 413 s-421 s, Oct. 1987.
7) Nonaka, K. and Kawahito, T. : The construction report on the Nagoya Harbour West Bridge , Bridge and foundation, Vol. 19, No. 5, pp. 22-30, 1985 (in Japanese).
8) Miki, C. et al. : Computer simulation studies on the fatigue load and fatigue design of highway bridges, Structural Eng. /Earthquake Eng., Vol. 2, No. 1, 1985.
9) Miki, C. et al. : The report of weight measurement of vehicles, Bridge and foundation, Vol. 21, No. 4, pp. 41-45, 1987 (in Japanese).
10) Kubo, Nakajima and Kameda : Field investigation of live loads on road birdges and study by a probabilistic model, Bridge and foundation, Vol. 20, No. 1, pp. 11-20, 1986 (in Japanese).
11) Makino, F. et al. : On the field investigation of traffic loads on bridges and distribution of live loads, Bridge and foundation, Vol. 19, No. 12, pp. 11-20, 1985 (in Japanese).
12) Wyatt, T. A. : A secondary stress in parallel wire suspension cables, ASCE, ST 7, pp. 39-59, 1960.
13) Fujino, Y. et al. : A stochastic study on effect of multi truck presence on fatigue damage on highway bridges, Structural Eng. /Earthquake Eng., Vol. 3, No. 2, pp. 457 s-467 s, Oct. 1986.
14) Fujino, Y. et al. : Effect of multiple presence of vehicles on fatigue damage on highway bridges, Proceedings of Structural Engineering, Vol. 33 A, pp. 775-785, Mar. 1987 (in Japanese).
15) Hirai, A. et al. : Steel Bridges Ⅲ, Chapter 8, Gihodo, 1967.

(Received January 31 1989)